A REVIEW OF AUTOMOTIVE THERMOELECTRIC GENERATOR

GOVIND MISHRA[1], SHUSHIL KUMAR SHARMA [2]
[1]B.E.scholar, D.MAT, Raipur, Chhattisgarh, India
[2] Assistant professor, D.MAT, Raipur, Chhattisgarh, India

Abstract- An automotive thermoelectric generator (ATEG) is a device that converts some of the waste heat of an internal combustion engine (IC) into electricity using the Seebeck Effect. A typical ATEG consists of four main elements: A hot-side heat exchanger, a cold-side heat exchanger, thermoelectric materials, and a compression assembly system. ATEGs can convert waste heat from an engine's coolant or exhaust into electricity. By reclaiming this otherwise lost energy, ATEGs decrease fuel consumed by the electric generator load on the engine. However, the cost of the unit and the extra fuel consumed due to its weight must be also considered.

Index Terms- Thermoelectric generator, Waste heat, Internal combustion engine, See beck Effect, Electricity, Fuel consumed.

1. INTRODUCTION

1.1 OVERVIEW

The main focus of energy conversion is on three conversion locations mainly exhaust gas pipe (EGP), exhaust gas recirculation (EGR) cooler, and retarder. The most significant factors for the waste heat quality are power density and temperature range.

The EGP is the target of the most automobile waste heat recovery related research. The exhaust system contains a large portion of the total waste heat in vehicle. The gas flow in exhaust gas pipe is relatively stable. Fig.1 shows that TEG utilizing the exhaust gas heat for operation. With exhaust temperatures of 973 K or more, the temperature difference between exhaust gas on the hot side and coolant on the cold side is close to 373 K.

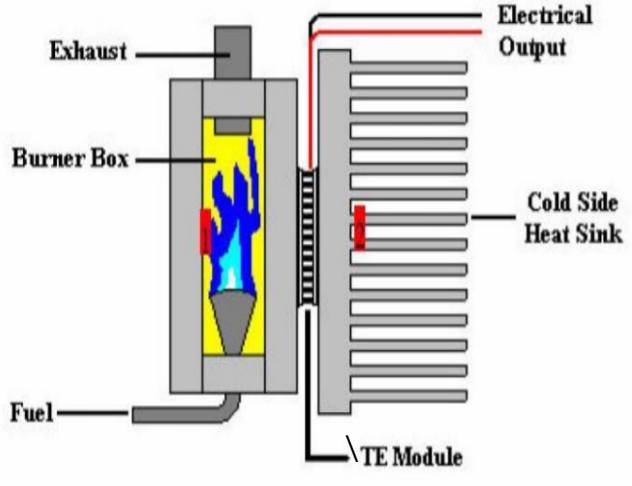

Fig.1 TEG utilizing the exhaust gas heat

This temperature difference is capable of generating 100-500W of electricity. In the water coolant based system, though the temperature is lower, it may be high enough to produce significant electricity for use in the vehicle when TEGs are attached.

The main advantage of EGR gas is large temperature difference. Since EGR gas comes directly from the cylinders, its temperature is in the range of 820 K-1050 K, which is similar to that in exhaust manifold. Considerable amount of heat. In the power plants and other industries there are lots of flue gases produced having significant amount heat. In the chimneys the temperature of flue gases would be around 373K which is the hot junction & the ambient air is cold junction having temperature 308 K. So there is temperature difference of 353 K. Applying the same technique to this it will gives output of 4.583 mV for one thermocouple loop so by adding these in series in large number we can generate large amount of electricity.

1.2 Case Study

1.2.1 GMC Sierra Pick-up Truck

In 2004, the Automobile Exhaust Thermoelectric Generator (AETEG) project was launched by Clarkson University and several companies, such as Delphi Harrison Thermal System, GM Power train Division and Hi-Z Technology, Inc. The purpose of the project is to perform a feasibility investigation for the application of thermoelectric generators on a GM pick-up truck, as well as to develop a commercial plan for the designed AETEG system. The device was targeting a power output of 330W, being supplied with heat from the exhaust and cooled by the conventional coolant circuit. A CAD model of the device can be seen in Fig.2. Efficiencies of the electronic device converting the electrically generated TEG in the order of 80-90%. The maximum amount of electricity created was 140 W to 225 W, with different types of configurations.

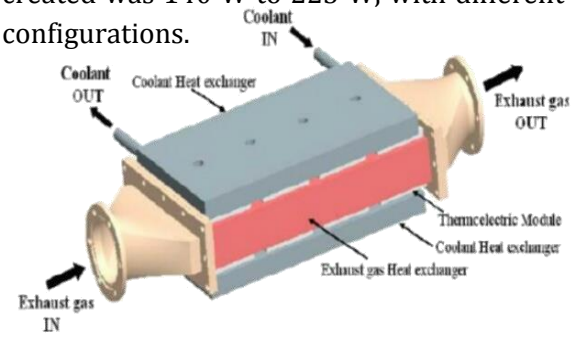

Fig.2 The CAD model of the assembled AETEG in GM pick-up truck project.

1.2.2 BMW Vision Efficient Dynamics Program

As a world leader in automobile industry, BMW launched its ATEG program Vision Efficient Dynamics in March 2009. The company develop pad a prototype vehicle (see Fig.3) fitted with a thermoelectric generator, based on Bismuth Telluride materials, for electric power production on board. The vehicle involved was BMW 530i. The power production reached levels of 200Wduring highway driving at 130km/h. The ZT-value was claimed to be around 0.4.However, there exist better materials already which yield a higher ZT-value, e.g. a PbTe-synthesis. Based on tests and observations, BMW predict potential fuel consumption savings in the order of 1-8% depending on driving condition. BMW claims future progress mainly depends on how well the laboratory demonstrated materials find their way to the commercial market.

Fig.3 BMW prototype vehicle using TEG waste heat recovery

WORKING PRINCIPLE

In ATEGs, thermoelectric materials are packed between the hot-side and the cold-side heat exchangers. The thermoelectric materials are made up of p-type and n-type semiconductors, while the heat exchangers are metal plates with high thermal conductivity.

The temperature difference between the two surfaces of the thermoelectric module(s) generates electricity using the Seebeck Effect. When hot exhaust from the engine passes through an exhaust ATEG, the charge carriers of the semiconductors within the generator diffuse from the hot-side heat exchanger to the cold-side exchanger as sown in Fig.4. The build-up of charge carrier's results in a net charge, producing an electrostatic potential while the heat transfer drives a current. With exhaust temperatures of 700°C (~1300°F) or more, the temperature difference between exhaust gas on the hot side and coolant on the

cold side is several hundred degrees. This temperature difference is capable of generating 500-750 W of electricity.

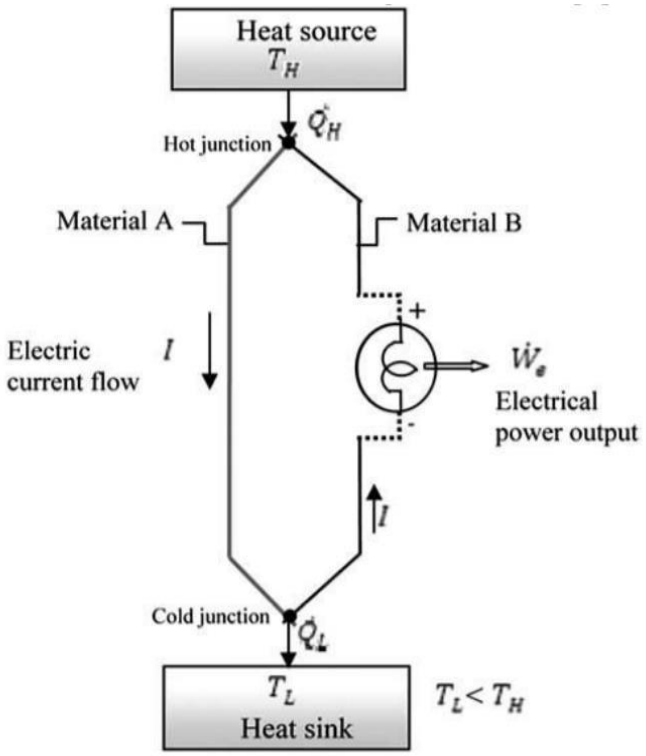

Fig.4 Principle of thermoelectric generator

2.1 Seebeck Effect

The Seebeck Effect is the conversion of temperature differences directly into electricity. It is a classic example of an electromotive force (emf) and leads to measurable currents or voltages in the same way as any other emf. Electromotive forces modify Ohm's law by generating currents even in the absence of voltage differences (or vice versa); the local current density is given by,

$$J = \sigma (-\Delta V + E_{emf})$$

Where, V the local voltage and σ is the local conductivity. In general the Seebeck effect is described locally by the creation of an electromotive field.

$$E_{emf} = -S \Delta T$$

Where S is the Seebeck coefficient (also known as thermo-power), a property of the local material, and ΔT is the gradient in temperature T.

2.2 Thermoelectric Principle of Operation

Thermoelectricity means the direct conversion of heat into electric energy, or vice versa. According to Joule's law, a conductor carrying a current generates heat at a rate proportional to the product of the resistance (R) of the conductor and the square of the current (I). A circuit of this type is called a thermocouple; a number of thermocouples connected in series are called a thermopile. To the Seebeck effect: If a current passes through a thermocouple, the temperature of one junction increases and the temperature of the other decreases, so that heat is transferred from one junction to the other. The rate of heat transfer is proportional to the current and the direction of transfer is reversed if the current is reversed.

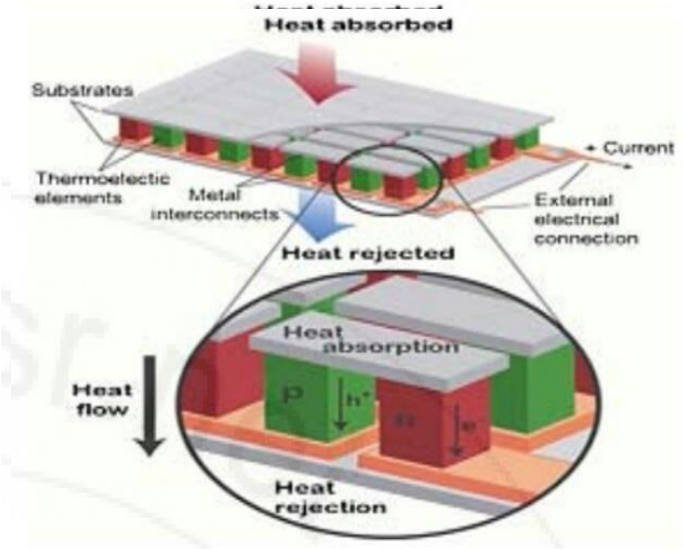

Fig. Thermionic Principle of Operation Jean C. A. Peltier discovered an effect inverse

The compression assembly system aims to decrease the thermal contact resistance between the thermoelectric modulz and the heat exchanger surfaces. In coolant-based ATEGs, the cold side heat exchanger uses engine coolant as the cooling fluid, while in exhaust-based

ATEGs, the cold-side heat exchanger uses ambient air as the cooling fluid.

2.3 Construction

Thermoelectric generator is a device that converts thermal energy directly into electrical energy.

The TEG structure is "sandwich like", with thermoelectric materials which are "sandwiched" by two heat exchanger plates at its ends respectively. One of the two exchangers is at high temperature, and hence, it is called the hot side of the TEG; while the other side is at lower temperature and is called the cold side of the TEG. There are electrical-insulate-thermal-conductive layers between the metal heat exchangers and the TE material of TEG. The two ends of n- and p-type legs are electrically connected by metal .The structure of TEG is as shown in fig.

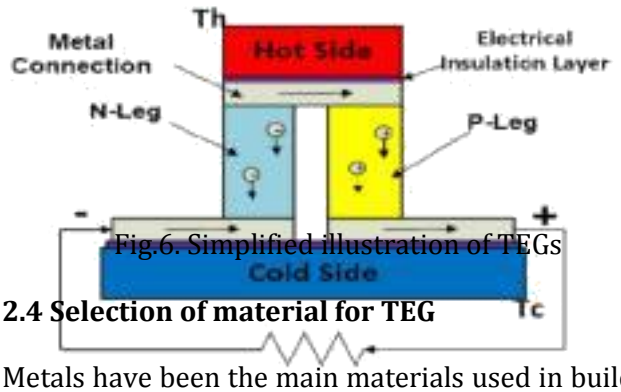

Fig.6. Simplified illustration of TEGs

2.4 Selection of material for TEG

Metals have been the main materials used in building TEGs, Despite metals' merit of high ratio of electrical to thermal conductivity, modern TE materials includes 26 main semiconductors. The performances of TEGs are largely affected by the materials used. Hence, the selection and combination of TE materials is important for the design of a good TEG. It is necessary to examine and compare the various TE materials. TEGs mainly have segmented structures. Within a segmented structure, each material should be used in their best temperature range (BTR).

Table 2.4.1 N-type material groups by best temperature range.

Group	Material	BTR
Hot Side Material (700 K-1000 K)	CoSb3, PbTe, SiGe	650-1100, 600-850>1000
Cold Side Material (300 K 400K)	Bi2Te3	<350

Table 2.4.2 P-type material groups by best temperature range.

Group	Material	BTR
Hot Side Material (700 K-1000k)	Zn4Sb3, CeFe4Sb12, SiGe, TAGS	>600 >850 900-1300, 650-800
Cold Side Material (300 K-400 K)	Bi2Te3	<450

S.no.	TEG Material	Temperature Range

1.	Alloys based on Bismuth (Bi) in combinations with Antimony(An), Tellurium (Te) or Selenium (Se)	Low temperature up to 450K
2.	Materials based on alloys of Lead (Pb)	Intermediate temperature up to 850K
3.	Material based on Si-Ge alloys	Higher temperature upto1300K

Table 2.4.3 Material used in TEG with range of temperature.

2.5 Segmentation

In modern TEGs, two or more types of materials are usually used in one leg, to increase the efficiency of the TEG. This approach of increasing TE couple efficiency is called as segmentation. It is a thumb rule that, the compatibility factors of materials within the same leg cannot differ by a factor of 2 or more. If this rule is violated, the maximum efficiency can be decreased by segmentation. Thus, the compatibility factor *s*, is one of the important considerations while selecting TE materials.

Table 2.5.1 Property of different material.

Properties		Hastelloy	Steel	Stainless steel	Copper	Duralumin
Type		–	AISI 1010	AISI 302	99.9 Cu + Ag	–
Melt point [K]		1533	1670	1670	1293	923
Density [kgm^{-3}]		8300	7830	8055	8950	2770
k [$Wm^{-1}K^{-1}$]	T = 294 K	9.1	–	–	–	–
	T = 300 K	-	64	15	386	174
	T = 473 K	14.1	–	–	–	–
	T = 500 K	–	54	19	–	188
k_p [$Jkg^{-1}K^{-1}$]	T = 294 K	486	–	–	–	–
	T = 300 K	–	434	480	385	875

METHODOLOGY

A simple model system is generated to derive explicit thermoelectric effect expressions for Seebeck. The model applies an n-type semiconductor junction with two different charge-carrier concentration *nL* and *nR*. Seebeck effect are calculated by applying a reversible closed Carnot cycle.

Seebeck's EMF of two junctions at different temperatures T_H and T_C is:

$$V= -S(T_H-T_C)$$

3.1 Background.

The Seebeck effect is the production of EMF, electromotive force, with junctions of two different conductors. Two junctions connected back to back are held at two different temperatures TH and TC and an EMF *V* appears between their free contacts:

$$V= -S(T_H-T_C) \quad (1)$$

Seebeck's coefficient calculated by the model is:$S=k \ln(n_L/n_R)$

S is Seebeck's coefficient.

The purpose of this page is to generate a simple system and calculate for it explicit expressions of the thermoelectric coefficients. Electrons in conductors occupy energy levels in pairs of opposite spins. Lower levels are fully occupied and upper levels are empty and the level population is determined by Fermi-Dirac statistics. In order to move in the conductor an electron that occupies some level must be scattered to an empty level. For this reason low energy electrons do not contribute to electric current because their nearby levels are all occupied. The Fermi level is the energy where the electron occupation probability is 0.5. Only electrons with energies near this level contribute to the current. The Maxwell-Boltzmann distribution of the electron velocity is not applicable in this case.

Semiconductor crystals are a special case. A fully occupied valence band is separated from an empty

conduction band in these materials by a forbidden gap without energy levels in it. If the gap is large enough direct thermal excitation of electrons from band to band is negligible and the material will be an insulator. Introduction of donors to the material will add electrons to the conduction band and make it *n*-type. Acceptors will add holes to the valence band and make it *p*-type. A donor atom has an extra electron, compared to a crystal atom, at a level just below the bottom of the conduction band and it will be thermally transferred to the conduction band where it is free to move. An acceptor atom has one less electron just above the valence band. An Electron caught by the acceptor will leave a free moving hole in the valence band. Practically, if the donor level is shallow, then all the donors will be ionized in *n*-type material. So that the density of free moving electrons is equal to the donor density. Similarly, the density of free moving holes is equal to the acceptor density in *p*-type material.

If the doping levels are not too high the charge carrier density, either of electrons or holes, will be lower than the energy level density within the bands. Each carrier may be scattered to many neighboring empty levels so that practically it is a free particle. The Maxwell-Boltzmann velocity distribution will then be applicable to the carriers.

3.2 Thermal Energy of a Particle

The average kinetic energy is calculated by summing all the squared velocities over all directions in space in a spatial angle of 4π determined by a declination angle θ, 0 to π and

azimuth angle of 2π. Each velocity is weighed by a distribution probability $f0(x, v, \theta)$:

$$<v^2>=\int f_0(x,v,\theta)\ |\boldsymbol{v}|^2 d^3\boldsymbol{v}, \qquad (2)$$

where $v = |\boldsymbol{v}|$ and $d^3\boldsymbol{v}=2\pi v^2 dv Sin(\theta)d\theta$.

Maxwell-Boltzmann distribution is:

$$f_0(v)=(m/2\pi kT)(3/2)e^{-mv2/2kT}, \qquad (3)$$

where the pre-exponential factor in (3), determined by the condition

$\int_0^\infty 4\pi v^2 f_0 dv=1$, is applied to the calculation of $<v^2>$. By transforming to a dimensionless variable $x=(m/2kT)^{1/2}v$, and using the integrals in appendix A :

$$<v^2>=4\pi\int f_0(v)v^4 dv=3kT/m. \qquad (4)$$

The average kinetic energy is:

$$m<v^2>/2=(3/2)T. \qquad (5)$$

3.3 Contact Potential

Consider two pieces of *n*-type semiconductor with higher nL and lower *nR* electron densities, where *nL* and *nR* are equal to the corresponding donor densities. Therefore, these densities are temperature independent. If the two pieces are brought into contact to form a junction, electrons will start to diffuse from the left higher *nL* to the right lower *nR* density. The diffusion generates a space charge region, electric field, and potential difference *Vc* between the two pieces, that stops further electron diffusion. *Vc* is the contact potential. It is not directly measureable by a voltmeter, for example, because the voltmeter probes make their own contact potentials with the two ends of the junction. The sum of all the junction potentials is then zero.

If the two pieces are separated after being in contact, their capacity will drop, the voltage between them will go up and it will then be measureable. Methods that measure the contact potential are based on this phenomenon is calculated:

$$e^{-eVc/kT}=n_R/n_L, \qquad (6)$$

or (16):

$$Vc=(kT/e)\ln(n_L/n_R). \qquad (7)$$

e is the electron charge and *k* is Boltzmann's constant.

It is assumed that the junction is perpendicular to the *x*-direction, and that the depth of the space charge layer in it is small compared to the electron's mean free path. The thermal velocity of electrons on the left side must have a minimal component *vx* in order to overcome the potential barrier and cross to the right side: (1/2) [2]. Electrons on the right side do not have a barrier for crossing back to the left. An electron that crosses the junction from left to right, will be slowed by the electric field and lose energy *eVc*. This energy will be thermally regained from its vicinity. An electron moving in the opposite direction will be accelerated by the field and thermally deliver the field-gained energy to its vicinity.

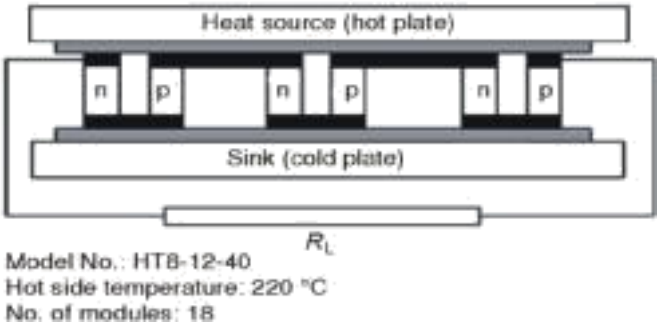

Fig.7. TEG connected to the load

The current density through the contact will be:

$$J_n=\int_{v_x>v_0} f_0(v)v_x d^3v+\int_{v_x<v_0} f_0(v)v_x d^3v = J_n^2 - J_n^1, \quad (8)$$

where: $v_0=(2eV_c/m)^{1/2}$.

It is convenient to use here Cartesian coordinates $d^3\boldsymbol{v}=dv_x dv_y dv_z$. By inserting the Maxwell-Boltzmann distribution (3) the current will be:

$$J_n^2=n\left(\frac{m}{2\pi kT}\right)^{3/2}\int_0^\infty e^{\alpha_z}dv_z\int_0^\infty e^{\alpha_y}dv_y\int_0^\infty e^{\alpha_x}v_x dv_x \quad (9)$$

$$J_n^1=n\left(\frac{m}{2\pi kT}\right)^{3/2}\int_{-\infty}^0 e^{\alpha_z}dv_z\int_{-\infty}^0 e^{\alpha_y}dv_y\int_{-\infty}^0 e^{\alpha_x}v_x dv_x \quad (10)$$

where: $\alpha_i=-mv_i^2/(2kT)$, $i = x, y, z$.

Using the formulas in appendix-A, the integrals will be:

$$\int_0^\infty e^{\alpha_i}dv_i=(\pi kT/m)^{1/2}, \quad (11)$$

$$\int_{v_0}^\infty e^{\alpha_x}v_x dv_x=(kT/m)^{-eVc/kT}, \quad (12)$$

$$\int_{-\infty}^0 e^{\alpha_x}v_x dv_x=(kT/m). \quad (13)$$

The overall current will be:

$$J_n=J_n^2 - J_n^1=(kT/8\pi m)^{1/2}n_L(e^{-eVc/kT}-n_R/n_L). \quad (14)$$

For equilibrium, $J_n= 0$, the potential difference at the contact will be:

$$e^{-eVc/kT}=n_R/n_L \quad (15)$$

or:

$$V_c=(kT/e)\ln(n_L/n_R). \quad (16)$$

If an external voltage source *V* is connected to the system, and the voltage falls on the junction, the current will be:

10

$$J_n=(kT/8\pi m)^{(1/2)}n_L(e^{e(V-Vc)/kT}-n_R/n_L), \quad (17)$$

or, by (28):

$$J_n=(kT/8\pi m)^{(/12)}n_R(e^{eV/kT}-1). \quad (18)$$

This formula is the *I*–*V* diode equation.

3.4 Charge Flow in a Semi-Conductor with Temperature Gradient

The electric current through a semi-conductor with a temperature gradient is calculated by applying Boltzmann transport equation. This equation yields expressions for the currents that are similar to Onsager's linear equations that relate forces to flows, but with the advantage that there are no unknown linear coefficients. If the charge carrier density does not depend on the position, then the electric current J_q will be:

$J_q=[E-(k/2e)/dx]$ (19)

Whereσ is the electrical conductivity (40) and E is the electric field.

For zero current (19) may be integrated to yield:

$V=(k/2e)\Delta T.$ (20)

By using the values of k and e a voltage gradient of 43 microvolt/degree, independent of the charge density, is developed between the cold and hot ends of the conductor.

The charge flow within a conductor is calculated by application of Boltzmann transport equation. A temperature gradient along the x-coordinate is assumed.

(x,y) is a non-equilibrium distribution function that determines the probability of a particle within a system to be at some place x and to have some local thermal velocity $\boldsymbol{v}$. The Boltzmann transport equation expresses this global non-equilibrium distribution in terms of local equilibrium distributions f_0(x ,y). The equation enables application of properties of equilibrium systems to the study of a non-equilibrium system. The linear transport equation is:

$f(x,v,\theta)=f_0(x,v)-lCos(\theta)[(\partial f_0/\partial x)+(\boldsymbol{a}/v)(\partial f_0/\partial v)]$, (21)

Where l is the mean free path, $\boldsymbol{v}$ is the velocity vector, $v = |\boldsymbol{v}|$, and θ is the vector direction relative to the x-coordinate. $\boldsymbol{a}$ is the acceleration due to external force. For example, $\boldsymbol{a} = e\,\boldsymbol{E} / m$, where $\boldsymbol{E}$ is the electric field, e is the particle charge and m is its mass. Equation (21) is obtained from the classical linear transport equation [20] by replacing the relaxation time $\tau = l / v$.

The currents: A particle moving with a velocity $\boldsymbol{v}$ will cross a plane section of the conductor at x during a time Δt if its distance from the plane is less than ( ) . The particle current through a unit cross section at x is obtained by summing all the velocities in all directions (spatial angle of 4π). Each velocity weighed by the distribution probability:

$J_n=\int(x)f(x,v,\theta)vCos(\theta)d^3v$, (22)

where $d^3v=2\pi v^2dvSin(\theta)d\theta$. Substitution of the distribution function (21) into (22) yields the current:

$J_n=-(4\pi l/3)[(eE/m)\int n(x)(\partial f_0/\partial_v)v^2dv+\int n(x)(\partial f_0/\partial x)v^3dv]$,(23)

where the f_0 contribution in (23) is zero, and the trigonometric integral is $\int Cos(\theta)\,Sin(\theta)d\theta=2/3$.

Since the energy associated with each particle is $(1/2)v^2$ the energy current will be, by a similar calculation:

$J_u=(4\pi l/3)[(eE/m)\int n(x)(\partial f_0/\partial v)v^4dv+\int n(x)(\partial f_0/\partial x)v^5dv]$. (24)

The currents will now be calculated by applying the Maxwell-Boltzmann distribution (3). Since (by (3)), $\partial f_0/\partial v=-(mv/kT)f_0$, the particle current will be:

$J_n=-(4\pi l/3)[(eE/kT)-(d/dx)][n(x)\int(f_0)v^3dv)]$. (25)

Or, by transforming to a dimensionless variable $x=(m/2kT)^{1/2}v$, and using the integrals in appendix A:

$J_n=[4l/3(2\pi m)^{1/2}][eEn/(kT)^{1/2}-d(n(kT)^{1/2})/dx]$. (26)

Assuming that the charge density does not depend on the position, the current will be:

$J_n=[(4l/3)/(2\pi m)^{1/2}](1/kT)^{1/2}n[eE-(1/2)d(kT)/dx]$. (27)

The charge current will be $J_q=eJ_n$. A similar calculation yields the energy current:

$J_u=2[(4l/3)/(2\pi m)^{1/2}][(kT)^{1/2}eEn-d(nkT)^{3/2}/dx]$, (28)

or, by combining (26) and (28):

$J_u=2kTJ_n-2[(4l/3)/(2\pi m)^{1/2}]nkT^{½}d(kT)/dx$. (29)

Equation (29) expresses the energy current as a sum of two terms. The first is convection, the energy associated with the particle flow, and the second is heat conduction, which is proportional to the temperature gradient and independent of the particle current.

Equations (26), (29) may be applied to calculate the diffusivity, electrical and thermal conductivity, and to verify the Wiedemann-Franz law and Einstein relations.

For example, the electrical conductivity σ, defined by $J_q=eJ(dn/dx=0,dT/dx=0)=\sigma E$, is:

$\sigma=[(4l/3)/(2\pi m)^{1/2}]e^2n/(kT)^{1/2}$. (30)

Equations (26), (28) are similar to Onsager's linear equations that relate forces to flows, but have the advantage that they do not include unknown linear coefficients like Onsager's. The values of these coefficients may be obtained by comparing the two sets of equations.

Appendix A: Integrals

$\int_0^\infty x^n e^{-a2x2}dx=(n+1/2)/2a^{n+1}$. (31)

Γ is the gamma function: $(n)=(n-1)!$ (32)

$(x+1)=x\Gamma(x)$ (33)

$(x)\Gamma(x+1/2)=\Gamma(2x)\pi^{1/2}/2^{2x-1}$ (34)

$(1/2)=\pi^{1/2}$ (35)

$(3/2)=(1/2)\pi^{1/2}$ (36)

$(5/2)=(3/4)\pi^{1/2}$(37)

3.5 Thermoelectric Effects

Direct conversion of thermal to electrical energy is analysed by applying the original Carnot method to a junction device operating in a reversible four step closed cycle. The "Carnot machine" Two junctions of semiconductors are connected in parallel. The two semiconductors are in permanent contact in the left junction and are separated and moveable in the right junction. The distance between the separated pieces is externally controlled. The connecting wires are made of the same semiconductor material so that there is only one contact junction in the device.

The contact potential *Vc* within a junction is given by (7). Since the right junction parts are electrically charged, there will be attraction force between them. Changing the distance between them requires mechanical work. The machine operates in a four step cycle between a hotter heat-bath *TH* and a colder heat-bath *TC*.

In step-1 the machine is attached to the hot bath *TH*. The right upper part moves down isothermally toward the lower part with a constant junction potential *VH*. The increasing capacity of the right junction drives charge ΔQH that flows from the left contact junction that absorbs heat = from the hot bath (Peltier effect). The pieces of the right junction perform equivalent work on the external force that holds them in place.

In step-2 the machine is separated from the hot bath *TH* and the right upper part moves adiabatically further down toward the lower part. The machine cools down until the temperature drops to *TC* of the cold bath. The junction potential drops from *VH* to *VC*.

In step-3 the machine is attached to the cold bath *TC*. The upper part moves back isothermally with constant *VC* and recedes from the lower part. The decreasing capacity of the right junction drives charge ΔQC that flows in the opposite direction to step-1. The flow through the left junction delivers heat = to the cold bath (Peltier effect reversed direction) and the external force performs an equivalent work on the right junction.

In step-4 the machine is separated from the cold bath *TC*. The upper part continues to move up adiabatically and the machine heats up until it reaches the temperature *TH* of the hot bath. The junction potential goes up from *VC* to *VH*, its original state, and a full cycle is completed.

The adiabatic work done by the machine on the external force in step-2 is equal to the adiabatic work done by the external force on the machine in step-4. The EMF *V* of the machine is the work done by moving a unit charge in a complete closed cycle. This work is

equal to the sum of step-1 and step-3 for a unit charge *e*. using (7) the work will be:

3.6 Efficiency

Currently, ATEGs are about 5% efficient. However, advancements in thin-film and quantum well technologies could increase efficiency up to 15% in the future.

The efficiency of an ATEG is governed by the thermoelectric conversion efficiency of the materials and the thermal efficiency of the two heat exchangers. The ATEG efficiency can be expressed as:

$$\zeta OV = \zeta CONV \times \zeta HX \times \rho$$

Where:

- ζOV : The overall efficiency of the ATEG
- ζCONV : Conversion efficiency of thermoelectric materials
- ζHX: Efficiency of the heat exchangers

ρ : The ratio between the heat passed through thermoelectric materials to that passed from the hot side to the cold side.

EFFECT AND IMPACT ON SOCIOECONOMICAL DEVELOPMENT

The primary goal of ATEGs is to reduce fuel consumption. Forty percent of an IC engine's energy is lost through exhaust gas heat. By converting the lost heat into electricity, ATEGs decrease fuel consumption by reducing the electric generator load on the engine. ATEGs allow the automobile to generate electricity from the engine's thermal energy rather than using mechanical energy to power an electric generator. Since the electricity is generated from waste heat that would otherwise be released into the environment, the engine burns less fuel to power the vehicle's electrical components, such as the headlights. Therefore, the automobile releases fewer emissions.

Decreased fuel consumption also results in increased fuel economy. Replacing the conventional electric generator with ATEGs could ultimately increase the fuel economy by up to 4%.

The ATEG's ability to generate electricity without moving parts is an advantage over mechanical electric generators alternatives**.**

Advantages of Thermoelectric power generators over other technologies.

APPLICATION

As discussed in section 1 TEGs are used to develop electricity from waste heat released from EGP due to combustion of fuel and from power plants and some industries due to flue gases from chimneys.

Other applications of TEGs

Camping, portable coolers, cooling electronic components and small instruments. A camping/car type electric cooler can typically reduce the temperature by up to 20 °C (36 °F) below the ambient temperature. The cooling effect of Peltier heat pumps can also be used to extract water from the air in dehumidifiers. Climate-controlled jackets, wine coolers, thermal cyclers, satellites and spacecraft. Used for the synthesis of DNA by polymerase chain reaction (PCR).

CONCLUSION

Waste heat recovery entails capturing and reusing the waste heat from internal combustion engine and using it for heating or generating mechanical or electrical work. It would also help to recognize the improvement in performance and emissions of the engine if these technologies were adopted by the automotive manufacturers.

By using this thermoelectric system one can generate electricity from the high temperature difference and it is available at low cost. In heavy duty vehicles the smoke coming out of the exhaustion system will form the NOx gases which are major concern for the greenhouse gases. But because of this the temperature will come down of exhaust gases so, the formation of the NOx gases will be minimal.

If this concept of thermoelectric system is taken to the Nano level or micro level then there will be ample

amount of electricity can be generated which are just wasted into the atmosphere.

11. REFERENCES

1. Yang, Jihui. "Automotive Applications of Thermoelectric Materials". Journal ofElectronic Materials, 2009, VOL 38; page 1245
2. Snyder, G. J. Toberer, E. S. "Complex Thermoelectric Materials". Nature materials, 2008 , VOL 7; NUMBER 2, pages 105-114
3. "TEGs - Using Car Exhaust To Lower Emissions". Scientific Blogging. June 3, 2008
4. Laird, Lorelei. "Could TEG improve your car's efficiency?". DOE Energy Blog. August16, 2010
5. http://purl.access.gpo.gov/GPO/LPS118101
6. Ikoma, K., M.Munekiyo, K.Furuya, M.Kobayashi, T.Izumi, and K.Shinohara (1998). Thermoelectric Module and Generator for Gasoline Engine Vehicle. Proc. 17th International Conference on Thermoelectrics. Nagoya, Japan: IEEE pp. 464-467.
7. Yu, C. "Thermoelectric automotive waste heat energy recovery using maximum power point tracking". Energy Conversion and Management, 2008, VOL 50; page 1506
8. Stabler, Francis. "Automotive Thermoelectric Generator Design Issues". DOE Thermoelectric Applications Workshop.
9. Stabler, Francis. "Benefits of Thermoelectric Technology for the Automobile". DOE Thermoelectric Applications Workshop.o B. Neild, Jr., SAE-645A (1963).
10. Birkholz, U., et al. "Conversion of Waste Exhaust Heat in Automobile using FeSi2 Thermoelements". Proc. 7th International Conference on Thermoelectric Energy Conversion. 1988, Arlington, USA, pp. 124-128.
11. Thacher E. F., Helenbrook B. T., Karri M. A., and Richter Clayton J. "Testing an automobile thermoelectric exhaust based thermoelectric generator in a light truck" Proceedings of the I MECH E Part D Journal of Automobile Engineering, Volume 221, Number 1, 2007, pp. 95-107(13)
12. Kushch A., Karri M. A., Helenbrook B. T. and Richter Clayton J., "The Effects of an Exhaust Thermoelectric Generator of a GM Sierra Pickup Truck." Proceedings of Diesel Engine Emission Reduction (DEER) conference, 2004, Coronado, California,USA
13. LaGrandeur J., Crane D., Eder A., "Vehicle Fuel Economy Improvement through Thermoelectric Waste Heat Recovery", DEER Conference, 2005, Chicago, IL, USA
14. "2012 10Best: 10 Most Promising Future Technologies: Thermal Juice", *Car & Driver*, December 201Jaydeep. V. Joshi1 and N. M. Patel (2012), Thermoelectric system to generate electricity from waste heat of the flue gases, Advances in Applied Science Research, 3 (2):1077-1084
15. Basel I. Ismail, Wael H. Ahmed (2009), Thermoelectric Power Generation Using Waste heat as an Alternative Green Technology, Recent Patents on Electrical Engineering, 2, 27-39
16. Adavbiele A.S. (2013), Generation of Electricity from Gasoline Engine Waste Heat, Journal of Energy Technologies and Policy, Vol.3, No.5,
17. Peltier application notes 20050 SW 112th Ave. Tualatin, Oregon 97062
18. KTH Information and Communication Technology, Thermoelectric-Generator-Based DCDC Conversion Network for Automotive Applications. Master of Science Thesis Stockholm, Sweden 2011.Trita-ICT-EX-2011:58.Molanli
19. Ravikumar, N., Ramakrishna, K., Sitaramaraju, A. V., Thermodynamic Analysis of Heat Recovery Steam Generator in Combined Cycle Power Plant, *Thermal Science, 11* (2007), 4, pp. 143-156.
20. Polyzakis, A. L., *et al*., Long-Term Optimization Case Studies for Combined Heat and Power System, *Thermal Science, 13* (2009), 4, pp. 46-60.
21. Chammas, El., Clodic, R., Clodic, D., Combined Cycle for Hybrid Vehicles, *SAE Paper* No. (2005)- 01-1171.
22. Ramesh Kumar, C., Sonthalia, A., Goel, R., Experimental Study on Waste Heat Recovery from an IC Engine using Thermoelectric Technology, *Thermal science*, 15 (2011), 4, pp. 1011 – 1022.
23. Zhang, H., Wang, E., Ouyang, M., Fan, B., Study of Parameters Optimization of ORC for Engine Waste Heat Recovery, *Adv Mat Res* , Vols. 201-203 (2011), pp. 585-589.
24. Kadota, M., Yamamoto, K., Advanced Transient Simulation on Hybrid Vehicle using Rankine Cycle System, *SAE Paper* No. (2008)-01-0310.

25 Ringler, J., Seifert, M., Guyotot, V., Huebner, W., Rankine Cycle for Waste Heat Recovery of IC Engines, *SAE Paper* No. (2009)-01-0174.

26 Hountalas, D.T., Katsanos, C.O., Kouremenos, D.A., Study of Available Exhaust Gas Heat Recovery Technologies for HD Diesel Engine Applications, *Int. J. Altern Propul*, 1(2007), No. 2/3.

[27] Sharad Chandra Rajpoot, Prashant singh Rajpoot and Durga Sharma,"Summarization of Loss Minimization Using FACTS in Deregulated Power System", International Journal of Science Engineering and Technology research ISSN 2319-8885 Vol.03, Issue.05,April & May-2014,Pages:0774-0778.

[28] Sharad Chandra Rajpoot, Prashant Singh Rajpoot and Durga Sharma, "Voltage Sag Mitigation in Distribution Line using DSTATCOM" International Journal of ScienceEngineering and Technology research ISSN 2319-8885 Vol.03, Issue.11, April June-2014, Pages: 2351-2354.

[29] Sharad Chandra Rajpoot, Prashant Singh Rajpoot and Durga Sharma, "A typical PLC Application in Automation", International Journal of Engineering research and TechnologyISSN 2278-0181 Vol.03, Issue.6, June-2014.

[30] Sharad Chandra Rajpoot, Prashant Singh Rajpoot and Durga Sharma,"21st century modern technology of reliable billing system by using smart card based energy meter",International Journal of Science Engineering and Technology research,ISSN 2319-8885 Vol.03,Issue.05,April & May-2014,Pages:0840-0844.

[31] Prashant singh Rajpoot , Sharad Chandra Rajpoot and Durga Sharma,"wireless power transfer due to strongly coupled magnetic resonance", international Journal of Science Engineering and Technology research ISSN 2319-8885 Vol.03,.05,April & May-2014,Pages:0764-0768.

[32] Sharad Chandra Rajpoot, Prashant Singh Rajpoot and Durga Sharma," Power system Stability Improvement using Fact Devices",International Journal of Science Engineering and Technology research ISSN 2319-8885 Vol.03,Issue.11,June-2014,Pages:2374-2379.